PHYSICAL REVIEW D **92,** 025003 (2015)

Phase of the fermion determinant in QED_3 using a gauge invariant lattice regularization

Nikhil Karthik* and Rajamani Narayanan†

Department of Physics, Florida International University, Miami, Florida 33199, USA

(Received 8 May 2015; published 1 July 2015)

We use canonical formalism to study the fermion determinant in different three-dimensional Abelian gauge-field backgrounds that contain nonzero magnetic and electric flux in order to understand the nonperturbative contributions to the parity-odd and parity-even parts of the phase. We show that a certain phase associated with free fermion propagation along a closed path in a momentum torus is responsible for the parity anomaly in a background with nonzero electric flux. We consider perturbations around backgrounds with nonzero magnetic flux to understand the structure of the parity-breaking perturbative term at finite temperature and mass.

DOI: 10.1103/PhysRevD.92.025003 PACS numbers: 11.15.-q, 11.15.Yc, 12.20.-m

I. INTRODUCTION

Three-dimensional Euclidean Abelian gauge theory coupled to a two-component massless fermion by

$$\not{D}(\mathbf{A}) = \sigma_k(\partial_k + iA_k) \tag{1}$$

can induce a parity-breaking mass term for the gauge field in the form of a Chern-Simons action [1–3]

$$S = \frac{i\kappa}{4\pi}\int d^3x A_k F_k \quad \text{where } F_k = \epsilon_{kij}\partial_i A_j. \tag{2}$$

The mass term is gauge invariant in infinite volume provided the fields are assumed to vanish at infinity. This result has been shown in perturbation theory using the gauge invariant Pauli-Villars regularization [4].

Theories with $2N$ flavors of massless fermions can have a real and positive determinant with proper pairing of fermions. Vacuum energy arguments show that the $O(2N)$ symmetry breaks down to $O(N)\times O(N)$ symmetry [5] and it has been shown that dynamical masses are generated for fermions that do not break parity [6] in the large N limit. Recent calculations along the same lines using Schwinger-Dyson equations [7] attempt to identify the phase structure that separates one where dynamical masses are generated from others that do not. Numerical studies using staggered fermions [8–10] have been performed and condensates have been computed for theories that do not break parity, again with the aim of exploring the phase structure.

The gauge theory with one flavor of a two-component Dirac fermion can be regularized in a gauge invariant manner using the Wilson-Dirac operator [11–13]

$$D_w(\mathbf{U},M) = \not{D}_n(\mathbf{U}) - B(\mathbf{U}) + M,$$
$$\not{D}_n^\dagger(\mathbf{U}) = -\not{D}_n(\mathbf{U}), \qquad B^\dagger(\mathbf{U}) = B(\mathbf{U}), \tag{3}$$

where $\mathbf{U}$ is the U(1)-valued lattice link variable, $\not{D}_n(\mathbf{U})$ is the naive lattice fermion operator, $B(\mathbf{U})$ is the Wilson term that provides a mass of the order of cutoff for the doublers, and $0 \le M < 1$ is the mass in lattice units for the fermion. Perturbation theory computations [13] using Eq. (3) in infinite volume show that the coefficient of the induced Chern-Simons term in Eq. (2) is $\kappa = -1$ if $M > 0$, and $\kappa = -\frac{1}{2}$ if one takes the massless limit after taking the continuum limit. For negative fermion masses, we would use

$$D_w(\mathbf{U},-M) = -D_w^\dagger(\mathbf{U},M) = \not{D}_n(\mathbf{U}) + B(\mathbf{U}) - M$$
$$\text{for } 0 \le M < 1, \tag{4}$$

so that the induced parity-breaking terms as one approaches the massless limit from the positive and negative side are opposite in sign.

A theory with $2N$ flavors with N flavors obeying Eq. (3) and the other N flavors obeying Eq. (4) can be used for a numerical investigation of condensates that do not break parity. We can also consider theories with nondegenerate fermions and an arbitrary number of flavors, and study the effect of parity-breaking mass terms in the limit of a large number of flavors.

Consider the continuum limit in a lattice simulation where we take the number of lattice points denoted by $L\to\infty$. The continuum limit needs to be taken keeping the physical spatial extent l, the fermion mass m_{phys} and the temperature T constant as $L\to\infty$. In a lattice calculation, it is natural to instead consider the dimensionless temperature $t = lT$ and the dimensionless mass $m = lm_{\text{phys}}$ measured in units of the spatial extent, to be the parameters of the theory and keep them constant as $L\to\infty$. Since we study

*nkarthik@fiu.edu
†narayanr@fiu.edu

fermions on fixed gauge-field backgrounds, the coupling constant g^2 does not play a role in the present calculations. The induced gauge action in a fixed gauge-field background will be gauge invariant and it is of interest to study this outside perturbation theory before embarking on a full lattice simulation. Of particular interest is the phase of the fermion determinant which contains parity-violating terms. Consider, for example [14], a gauge-field background that has a nonzero magnetic flux,

$$\int F_3 dxdy = 2\pi q_3, \tag{5}$$

for the integer q_3, along with a nonzero Polyakov loop, $e^{i\int A_3 d\tau} = e^{i2\pi h_3}$. The associated Chern-Simons action is

$$S(h_3, q_3) = i\kappa\pi h_3 q_3, \tag{6}$$

and it has to remain invariant under the gauge transformation $h_3 \to (h_3 + 1)$. This implies that κ has to be an even integer [15–17] for this particular gauge-field background in a regularization that preserves gauge invariance under such "large" gauge transformations [18–20]. This does not match with $\kappa = -1$ or $\kappa = -\frac{1}{2}$ obtained in [13]. The effect of nonvanishing gauge fields at infinity on spontaneous and anomalous breaking of parity has also been addressed in [21]. In addition to the parity-violating contributions to the phase of the fermion determinant,

$$e^{i\Gamma(t,m,\mathbf{A})} = \lim_{L\to\infty} \frac{\det D_w(U,M)}{|\det D_w(U,M)|}, \tag{7}$$

in the continuum limit, there are also parity-preserving contributions of the form $e^{i\pi h(A)}$ where $h(A)$ are integers associated with zero crossings of the Wilson-Dirac operator [22–24].

As a precursor to studying the three-dimensional theory, consider the regularized result using Wilson-Dirac fermions in one dimension in comparison to the results obtained in [14,18–20,25]. The Wilson-Dirac fermion operator in one dimension is

$$D_w(U,M) = -1 + M + T, \tag{8}$$

where the translation operator T is $(T\psi)(k) = U(k)\psi(k)$ in terms of the one-dimensional link variable, $U(k)$. The only physical degree of freedom is the Polyakov loop,

$$W = \lim_{L\to\infty} \prod_{k=1}^{L} U(k) = e^{i2\pi h}, \tag{9}$$

and the fermion determinant in the continuum, assuming L to be even, is

$$\lim_{L\to\infty} \det D_w\left(U, \frac{m}{L}\right) = \begin{cases} e^{i2\pi h} - e^{-m} = \begin{cases} e^{i2\pi h} & m = \infty \\ 2\sin(\pi h) e^{i\pi h + i\frac{\pi}{2}} & m = 0_+ \end{cases} \\ e^{-i2\pi h} - e^{-m} = \begin{cases} 2\sin(\pi h) e^{-i\pi h - i\frac{\pi}{2}} & m = 0_- \\ e^{-i2\pi h} & m = -\infty. \end{cases} \end{cases} \tag{10}$$

The result matches with the one obtained in [19] using zeta function regularization and has the main features discussed before. It is invariant under the large gauge transformation $h \to (h+1)$ for all values of m. The part of the phase proportional to h in the massless limit is half of its value in the infinite mass limit. As far as the vacuum structure is concerned, the partition function for a two-flavor theory with masses m_1 and m_2 is

$$Z(m_1, m_2) = \begin{cases} e^{-(m_1+m_2)} & m_1, m_2 > 0 \\ e^{-(m_1-m_2)} + 1 & m_1 > 0;\ m_2 < 0, \end{cases} \tag{11}$$

showing that the theory with $m_1 > 0$ and $m_2 < 0$ is preferred over $m_1, m_2 > 0$.

The aim of this paper is to study the phase $\Gamma(t, m, \mathbf{A})$ in the continuum U(1) gauge-field background on a three-dimensional $l \times l \times \frac{1}{t}$ torus given by

$$\begin{aligned} A_1 &= \frac{2\pi q_2 t}{l}\tau + \frac{2\pi h_1}{l} + A_1^p, \\ A_2 &= \frac{2\pi q_3}{l^2}x + \frac{2\pi h_2}{l} + A_2^p, \\ A_3 &= \frac{2\pi q_1 t}{l}y + 2\pi h_3 t + A_3^p, \end{aligned} \tag{12}$$

where q_i are integers and they denote nonzero flux in the x, y and τ directions, $h_i \in [0,1]$ denotes torons generating nontrivial Polyakov loops, and the A_i^p's are perturbative fields that obey periodic boundary conditions. The associated *periodic* boundary conditions on fermions are

$$\begin{aligned} \psi(l, y, \tau) &= e^{-i\frac{2\pi q_3 y}{l}}\psi(0, y, \tau), \\ \psi(x, l, \tau) &= e^{-i2\pi q_1 \tau t}\psi(x, 0, \tau), \\ \psi\left(x, y, \frac{1}{t}\right) &= e^{-i\frac{2\pi q_2 x}{l}}\psi(x, y, 0). \end{aligned} \tag{13}$$

We refer to q_3 as magnetic flux, and q_1 and q_2 as electric flux. The naming is not relevant if only one of the three is nonzero, but we also consider cases with $q_1 \neq 0$, $q_2 \neq 0$ and $q_3 = 0$ in this paper and extract some results without completely resorting to numerical means. In addition, we numerically study the most general case with nonzero flux in all three directions. The phase splits into a parity-even and -odd part

$$\Gamma = \Gamma_{\text{even}} + \Gamma_{\text{odd}}, \tag{14}$$

with the parity-even part being

$$\Gamma_{\text{even}} = \pi(q_1 + q_2 + q_3) + \pi(q_1 q_2 + q_3 q_1 + q_2 q_3). \tag{15}$$

The first term can be absorbed by changing the boundary conditions of fermions but not both the first and second terms. In general, the parity-odd part is complicated, but it has a simple form in the case of zero temperature when we consider a τ-dependent perturbation on a static and spatially uniform magnetic field:

$$\Gamma_{\text{odd}} = -2\pi h_3 q_3 - \int d\tau d\tau' A_1^p(\tau) A_2^p(\tau') G(\tau - \tau'), \tag{16}$$

where the form factor $G(\tau)$ is an odd function of τ that depends on the fermion mass m and spatial torons. Our formulation on the lattice enables us to study $G(\tau)$ without making prior assumptions concerning the local or nonlocal nature of the induced gauge action. We study how the form factor becomes local in the limit of $m \to \infty$ and $m \to 0$.

The organization of the paper is as follows. We describe lattice gauge fields on a torus in Sec. II. In Sec. III, we derive an expression for the Wilson-Dirac fermion determinant in the lattice axial gauge allowing for nontrivial Polyakov loops using the canonical formalism [26]. In Sec. IV, we use the canonical formalism to study cases with uniform electric and magnetic fields, organized into subsections. Here, we explain the origin of the parity-even phase in Eq. (15). First, we present a conventional way to understand the parity breaking when there is only a nonzero magnetic flux. The zero crossings of the eigenvalues of the two-dimensional Dirac operator are responsible for the parity-breaking terms and the formula for the fermion determinant using lattice regularization matches the one from zeta function regularization [18,19]. We then consider the case where we have nonzero electric fluxes but zero magnetic flux. We show that the relevant quantity to obtain the parity-even part of the phase is associated with the propagation of a free fermion with continuously changing momentum along a closed loop in the torus in momentum space in a direction defined by $(q_2, -q_1)$. Finally, we turn on perturbations over static magnetic field backgrounds. For this, we develop second order perturbation theory within the canonical formalism in Sec. V and use it to study the parity-odd part of the induced effective action. The results of the perturbative analysis and the numerical extraction of the form factor G are presented in Secs. V A and V B.

II. GAUGE FIELD ON A TORUS

We work on an $L^2 \times \beta$ lattice for the sake of simplicity, which can be easily generalized to a spatially anisotropic lattice as well. We only consider lattices where both L and β are even; while the continuum physics is independent of this choice, it helps to simplify our calculations. The spatial volume of the lattice is defined as $V \equiv L^2$. The spatial lattice points are labeled by $\mathbf{x} = (x_1, x_2)$ with $1 \leq x_i \leq L$, and the temporal lattice points by k with $1 \leq k \leq \beta$. The dimensionless temperature in the continuum limit is

$$t = \lim_{L\to\infty} \frac{L}{\beta}. \tag{17}$$

The continuum space and Euclidean time variables are

$$(x, y) = \lim_{L\to\infty} \left(\frac{x_1}{L}, \frac{x_2}{L}\right) \quad \text{and} \quad \tau = \lim_{L\to\infty} \frac{k}{L}, \tag{18}$$

with $x, y \in [0, 1]$ and $\tau \in [0, \frac{1}{t}]$.

On this lattice, we introduce U(1) gauge fields using the gauge links $U_\mu(\mathbf{x}, k)$. In this work, we fix the gauge such that the temporal gauge links from $k = 1$ to $k = \beta - 1$ are set to identity. Nontrivial Polyakov loop variables in the τ direction are taken care of by the presence of $U_3(\mathbf{x}, \beta) = U_3(\mathbf{x})$. This partial gauge fixing enables us to develop the canonical formalism in Sec. III. We still have a remnant time-independent gauge symmetry, $g(\mathbf{x})$, under which

$$\begin{aligned} &U_i(\mathbf{x}, k) \to g^\dagger(\mathbf{x}) U_i(\mathbf{x}, k) g(\mathbf{x} + \hat{i}) \\ \text{and} \quad &U_3(\mathbf{x}) \to g^\dagger(\mathbf{x}) U_3(\mathbf{x}) g(\mathbf{x}). \end{aligned} \tag{19}$$

In this work, we consider only the gauge fields of the form in Eq. (12). An analogous Hodge decomposition is strictly true for any gauge fields in two dimensions. In three dimensions, one should consider these as specific background gauge fields used in order to probe the dependence of the fermion determinant on perturbative and nonperturbative aspects of the gauge field. The gauge fields in Eq. (12) are periodic only up to a gauge transformation with nontrivial winding. Since we do not require smoothness of the link variables on the lattice, such gauge fields along with fermions, which satisfy the boundary conditions in Eq. (13), can be incorporated using gauge links and fermions that are strictly periodic. For our gauge choice, the lattice gauge-field background corresponding to Eq. (12) is

$$\begin{aligned} U_1(\mathbf{x}, k) &= \begin{cases} e^{i\frac{2\pi q_2}{L\beta}k} e^{i\frac{2\pi h_1}{L} + iA_1^q} & \text{if } x_1 < L \\ e^{i\frac{2\pi q_2}{L\beta}k - i\frac{2\pi q_3}{L}x_2} e^{i\frac{2\pi h_1}{L} + iA_1^q} & \text{if } x_1 = L, \end{cases} \\ U_2(\mathbf{x}, k) &= e^{i\frac{2\pi q_3}{L^2}x_1 - i\frac{2\pi q_1}{\beta L}k} e^{i\frac{2\pi h_2}{L} + iA_2^q}, \\ U_3(\mathbf{x}) &= e^{-i\frac{2\pi q_2}{L}x_1 + i\frac{2\pi q_1}{L}x_2} e^{i2\pi h_3}. \end{aligned} \tag{20}$$

The various background gauge fields we study in this paper are instances of the above equation.

III. CANONICAL FORMALISM

The partial gauge fixing defined in Sec. II naturally allows for the development of the Hamiltonian or the canonical formalism [26]. Let $T_i(k)$ be the parallel transporters along spatial directions at a fixed Euclidean time, k:

$$[T_j(k)\psi](\mathbf{x}) \equiv U_j(\mathbf{x},k)\psi(\mathbf{x}+\hat{j}), \tag{21}$$

and let T_3 defined as

$$[T_3\psi](\mathbf{x}) \equiv U_3(\mathbf{x})\psi(\mathbf{x}) \tag{22}$$

be the parallel transporter that connects $k=\beta$ and $k=1$. In this gauge-field background, the Wilson-Dirac fermion operator is

$$D^{kk'}(M) = \left[-3+M+\frac{1}{2}\sum_{i=1}^{2}[(\sigma_i+1)T_i(k)-(\sigma_i-1)T_i^\dagger(k)]\right]\delta^{k',k}+\frac{1}{2}\begin{cases}[(\sigma_3+1)\delta^{k',2}-(\sigma_3-1)T_3^\dagger\delta^{k',\beta}] & \text{if } k=1\\ [(\sigma_3+1)\delta^{k',k+1}-(\sigma_3-1)\delta^{k',k-1}] & \text{if } 1<k<\beta\\ [(\sigma_3+1)T_3\delta^{k',1}-(\sigma_3-1)\delta^{k',\beta-1}] & \text{if } k=\beta,\end{cases} \tag{23}$$

where the second term takes care of the periodicity in the temporal direction. In this way, we have managed to write the Dirac operator using operators defined on two-dimensional time slices. The Wilson mass M is such that $|M|<1$. It is related to the physical mass m in the units of box length as

$$m \equiv ML. \tag{24}$$

By using the following set of Pauli matrices,

$$\sigma_1=\begin{pmatrix}0 & 1\\ 1 & 0\end{pmatrix},\quad \sigma_2=\begin{pmatrix}0 & -i\\ i & 0\end{pmatrix},\quad \sigma_3=\begin{pmatrix}1 & 0\\ 0 & -1\end{pmatrix}, \tag{25}$$

the Wilson-Dirac operator D can be written in the matrix form as

$$D(M)=\begin{pmatrix}-B_1 & C_1 & 1 & 0 & \cdots & \cdots & 0 & 0\\ -C_1^\dagger & -B_1 & 0 & 0 & \cdots & \cdots & 0 & T_3^\dagger\\ 0 & 0 & -B_2 & C_2 & \cdots & \cdots & 0 & 0\\ 0 & 1 & -C_2^\dagger & -B_2 & \cdots & \cdots & 0 & 0\\ \vdots & \vdots & \vdots & \ddots & \ddots & \ddots & \vdots & \vdots\\ \vdots & \vdots & \vdots & \vdots & \ddots & \ddots & \ddots & \vdots\\ T_3 & 0 & 0 & 0 & \cdots & \cdots & -B_\beta & C_\beta\\ 0 & 0 & 0 & 0 & \cdots & \cdots & -C_\beta^\dagger & -B_\beta\end{pmatrix}, \tag{26}$$

where

$$B_k \equiv 3-M-\frac{1}{2}\sum_{j=1}^{2}(T_j(k)+T_j^\dagger(k)),$$
$$C_k \equiv \frac{1}{2}(T_1(k)-T_1^\dagger(k))-\frac{i}{2}(T_2(k)-T_2^\dagger(k)). \tag{27}$$

Note that B_k is a positive definite operator for $|M|<1$. We closely follow [27] in order to obtain an expression for the determinant of D. We first cyclically permute the columns to the left. This gives a matrix

$$D'(M)=\begin{pmatrix}\alpha_1 & 0 & 0 & \cdots & \cdots & 0 & \gamma_1 Y\\ \gamma_2 & \alpha_2 & 0 & \cdots & \cdots & 0 & 0\\ 0 & \gamma_3 & \alpha_3 & \cdots & \cdots & 0 & 0\\ \vdots & \vdots & \vdots & \ddots & \ddots & \vdots & \vdots\\ \vdots & \vdots & \vdots & \ddots & \ddots & \vdots & \vdots\\ 0 & 0 & 0 & \cdots & \cdots & \alpha_{\beta-1} & 0\\ 0 & 0 & 0 & \cdots & \cdots & \gamma_\beta & \alpha_\beta X\end{pmatrix}, \tag{28}$$

where

$$\alpha_k \equiv \begin{pmatrix}C_k & 1\\ -B_k & 0\end{pmatrix},\qquad \gamma_k \equiv \begin{pmatrix}0 & -B_k\\ 1 & -C_k^\dagger\end{pmatrix},$$
$$X \equiv \begin{pmatrix}1 & 0\\ 0 & T_3\end{pmatrix},\qquad Y \equiv \begin{pmatrix}T_3^\dagger & 0\\ 0 & 1\end{pmatrix}. \tag{29}$$

Using the formula for the determinant of the above matrix from [27], we arrive at

$$\det D(M) = \left[\prod_{j=1}^{\beta}\det\alpha_j\right]\det\left[X-\left(\prod_{k=\beta}^{1}\mathcal{T}_k\right)Y\right], \tag{30}$$

where the Hermitian transfer matrix $\mathcal{T}_k$ associated with propagating the fermion across the kth slice is

$$\mathcal{T}_k \equiv -\alpha_k^{-1}\gamma_k = \begin{pmatrix}B_k^{-1} & -B_k^{-1}C_k^\dagger\\ -C_kB_k^{-1} & C_kB_k^{-1}C_k^\dagger + B_k\end{pmatrix}. \tag{31}$$

The final expression for the fermion determinant is

$$\det D(M) = \left(\prod_{j=1}^{\beta} \det B_j\right) \det T_3 \det \mathcal{H}$$

$$\text{where } \mathcal{H} \equiv \mathbf{1} - \left(\prod_{k=\beta}^{1} \mathcal{T}_k\right) T_3^{\dagger}. \tag{32}$$

This is the main formula that we use repeatedly in order to understand the phase of the determinant Γ in this paper. Since B_j is positive definite, the phase becomes

$$\exp(i\Gamma) = \frac{\det D(M)}{|\det D(M)|} = \det T_3 \frac{\det \mathcal{H}}{|\det \mathcal{H}|}. \tag{33}$$

If the ξ_i's are the $2V$ eigenvalues of $\prod_{k=\beta}^{1} \mathcal{T}_k T_3^{\dagger}$, then

$$\exp(i\Gamma) = \det T_3 \prod_{i=1}^{2V} \frac{1-\xi_i}{|1-\xi_i|}. \tag{34}$$

The positivity of the Hermitian transfer matrices $\mathcal{T}_k$ follow from the positivity of B_k since

$$\begin{aligned} &(u^{\dagger} \quad v^{\dagger}) \mathcal{T}_k \begin{pmatrix} u \\ v \end{pmatrix} \\ &= (u - C_k^{\dagger} v)^{\dagger} B_k^{-1} (u - C_k^{\dagger} v) + v^{\dagger} B_k v > 0. \end{aligned} \tag{35}$$

In addition, they satisfy the *unitarity* property $\det \mathcal{T}_k = 1$.

A. Free field theory

In this subsection, we find the eigenvalues and eigenvectors of $\mathcal{T}$ (we can drop the subscript k) for free field theory, where all the gauge links are set to identity. The momenta p_1 and p_2 in the xy plane are

$$p_i = \frac{2\pi n_i}{L} \quad \text{where } n_i = 0, 1, \ldots L-1. \tag{36}$$

When expressed in this momentum basis, both B and C are the numbers

$$b = 1 - M + 2\sum_{j=1}^{2} \sin^2 \frac{p_j}{2}$$

$$\text{and} \quad c = i \sin p_1 + \sin p_2, \tag{37}$$

respectively. Thus $\mathcal{T}$ becomes

$$\mathcal{T}(n_1, n_2) = \begin{pmatrix} \frac{1}{b} & -\frac{c^*}{b} \\ -\frac{c}{b} & b + \frac{|c|^2}{b} \end{pmatrix}. \tag{38}$$

The eigenvalues of $\mathcal{T}(n_1, n_2)$ are $e^{\pm\lambda_p}$ with

$$\lambda_p = \cosh^{-1} \frac{1 + b^2 + |c|^2}{2b}. \tag{39}$$

The corresponding normalized eigenvectors for the zero mode (0, 0) and the doubler modes $(\pi, 0)$, $(0, \pi)$ and (π, π) are

$$|p+\rangle = \begin{pmatrix} 1 \\ 0 \end{pmatrix} \quad \text{and} \quad |p-\rangle = \begin{pmatrix} 0 \\ 1 \end{pmatrix} \quad \text{when } b < 1; \tag{40}$$

if $b > 1$, the above $|p+\rangle$ and $|p-\rangle$ get interchanged. For other generic modes

$$|p\pm\rangle = \frac{1}{\sqrt{|c|^2 + (1 - e^{\pm\lambda_p} b)^2}} \begin{pmatrix} c^* \\ 1 - e^{\pm\lambda_p} b \end{pmatrix}. \tag{41}$$

It is straightforward to extend the free theory results to a case where uniform spatial torons h_1 and h_2 are present. For this, one replaces $\mathcal{T}(n_1, n_2)$ by $\mathcal{T}(n_1 + h_1, n_2 + h_2)$.

IV. GAUGE-FIELD BACKGROUNDS WITH UNIFORM ELECTRIC AND MAGNETIC FIELDS

This section is devoted to gauge-field backgrounds with constant and uniform electric as well as magnetic fields i.e., nonzero q_1, q_2 and q_3. We first consider the case when $q_1 = q_2 = 0$ and assume that $h_3 \neq 0$. This is a standard example to understand the role of large gauge transformation in the parity-odd part of the induced action [14,18,19,25] and we will show that the results using the lattice formulation are consistent with zeta function regularization. Next, we consider the case of static electric fields ($q_1 \neq 0$, $q_2 \neq 0$ and $q_3 = 0$) by reducing the problem to a free fermion propagation with continuously changing momentum along a closed loop in a two-dimensional momentum torus. Apart from providing a different perspective to the constant magnetic field case, this also leads to an understanding of a parity-even phase $\pi q_1 q_2$. The last subsection deals with a numerical study of the general case where both the electric and magnetic fields are present.

A. Uniform and static magnetic field

Let us consider a gauge-field background with only a uniform magnetic field q_3 and the toron h_3. In this case, the matrices $\mathcal{T}_k = \mathcal{T}$ are time independent. The eigenvalues of $\mathcal{T}$ can be written as $e^{\pm\lambda_i}$ due to its positivity. The matrix $\mathcal{H}$ for this static case becomes

$$\mathcal{H}_{\text{st}} \equiv \mathbf{1} - \mathcal{T}^{\beta} e^{-i2\pi h_3}, \tag{42}$$

and its eigenvalues $1 - \xi_i^{\pm}$ are given by

$$\xi_i^{\pm} = e^{\pm\beta\lambda_i^{\pm} - i2\pi h_3}. \tag{43}$$

It is known [28] that q_3 eigenvalues of $\mathcal{T}$ cross unity as a function of mass when a nonzero topological charge q_3 is present; when $m > 0$, there are $V + q_3$ eigenvalues e^{λ^+}, and $V - q_3$ eigenvalues $e^{-\lambda^-}$ with $\lambda^\pm > 0$. The determinant of $\mathcal{H}_{\rm st}$ expressed in terms of these eigenvalues is

$$\det \mathcal{H}_{\rm st} = \prod_{i=1}^{V+q_3} (1 - e^{-i2\pi h_3 + \frac{L}{t}\lambda_i^+}) \prod_{j=1}^{V-q_3} (1 - e^{-i2\pi h_3 - \frac{L}{t}\lambda_j^-}). \tag{44}$$

Using Eq. (32), the phase of the determinant is

$$\Gamma = \pi q_3 - 2\pi h_3 q_3 + \sum_{i=1}^{V+q_3} \mathrm{Im}\log(1 - e^{i2\pi h_3 - \frac{L}{t}\lambda_i^+}) + \sum_{j=1}^{V-q_3} \mathrm{Im}\log(1 - e^{-i2\pi h_3 - \frac{L}{t}\lambda_j^-}). \tag{45}$$

The first term πq_3 is parity even, and it could be absorbed by changing $h_3 \to h_3 + \frac{1}{2}$. This formula is explicitly gauge invariant under a large gauge transformation $h_3 \to h_3 + 1$ and is a consequence of the gauge invariant regularization. At any finite fermion mass, all the $L\lambda_i^\pm$'s have nonzero finite continuum limits. At zero temperature, all the exponentials vanish leaving only the first two terms which do not depend on the fermion mass.

In order to check consistency with the results from zeta function regularization in [18,19], we computed Γ for several values of $m = ML$ and several values of $t = \frac{L}{\beta}$. For the different Γ that we computed at finite L, the mass term used in the zeta function regularization would correspond to

$$\frac{m_\zeta(L)}{t} = \ln \frac{\tan\Gamma}{\cos 2\pi h_3 \tan\Gamma - \sin 2\pi h_3}. \tag{46}$$

We extracted the continuum limit of m_ζ by fitting the results for $L = 20, 22, \ldots, 48, 50$ using a polynomial in $\frac{1}{L}$. We verified that the extracted value for m_ζ matches with m quite well. Our checks were made in the range $m \in [0.2, 1.0]$ and $t \in [0.1, 3]$. We show an example of the L dependence of m_ζ in Fig. 1 using $m = 0.7$ and $t = 1$. The continuum limit of m_ζ is seen to match with the m used in our lattice calculation.

B. Uniform and static electric fields

At any finite nonzero temperature and finite volume, it is possible to have spatially uniform and static electric fields, i.e., nonzero q_1 and q_2 which are integers. Also, q_1 and q_2 need not have the same value. In this subsection, we consider this case of nonzero electric fields, but with no

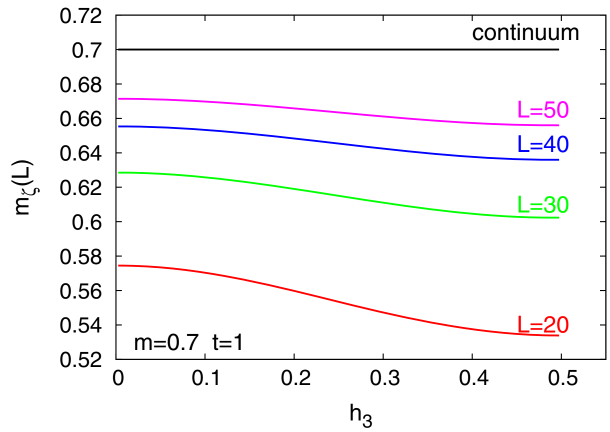

FIG. 1 (color online). The continuum limit of m_ζ [refer to Eq. (46)] at various h_3 is shown for $m = 0.7$ and $t = 1$. The spatial lattice extent L is specified on top of each curve. The continuum limit of m_ζ obtained by $1/L$ extrapolation is shown by the topmost black line. This continuum limit matches with $m = 0.7$ at all h_3.

magnetic field. The lattice gauge-field background in Eq. (20) reduces to

$$U_1(\mathbf{x}, k) = e^{i\frac{2\pi q_2}{L\beta}k},$$
$$U_2(\mathbf{x}, k) = e^{-i\frac{2\pi q_1}{\beta L}k},$$
$$U_3(\mathbf{x}) = e^{-i\frac{2\pi q_2}{L}x_1 + i\frac{2\pi q_1}{L}x_2}. \tag{47}$$

We focus on the parity-even phase arising from this configuration. At any time slice, the above U_1 and U_2 act like time-dependent torons h_1 and h_2 whose effect is to offset the momentum. Switching to the momentum basis and using the replacement $n_i \to n_i + h_i$, the two-dimensional transfer matrix becomes

$$\mathcal{T}_k^{n,s} = \mathcal{T}\left(n_1 + q_2\frac{k}{\beta}, n_2 - q_1\frac{k}{\beta}\right)\delta_{n_1,s_1}\delta_{n_2,s_2}, \tag{48}$$

where $\mathcal{T}$ is given by Eq. (38) for the case with torons. The n and s are the momentum indices. The product of these matrices is diagonal in momentum space and it is denoted as t_{n_1,n_2},

$$\left[\prod_{k=\beta}^{1}\mathcal{T}_k\right]^{n,s} \equiv \delta^{n_1,s_1}\delta^{n_2,s_2}t_{n_1,n_2}. \tag{49}$$

Since T_3 is already in a definite momentum $(-q_2, q_1)$, it becomes $\mathbf{1}\delta^{n_1,s_1-q_2}\delta^{n_2,s_2+q_1}$. Thus,

$$\left[\prod_{k=\beta}^{1}\mathcal{T}_k\mathcal{T}_3\right]^{n,s} = t_{n_1,n_2}\delta^{n_1-q_2,s_1}\delta^{n_2+q_1,s_2}. \tag{50}$$

We block diagonalize the above matrix in the following way. Starting from an arbitrary momentum (n_1, n_2), we create a cycle $\mathcal{C}$ by moving to $(n_1 - q_2, n_2 + q_1)$, then to $(n_1 - 2q_2, n_2 + 2q_1)$ and so on till we are back at (n_1, n_2). This will occur after P steps when both Pq_2 and Pq_1 become multiples of L. We refer to P as the cycle length and this is fixed given q_1, q_2 and L. The cycle $\mathcal{C}$ corresponds to a $P \times P$ block, and it has the following structure:

$$\left[\prod_{k=\beta}^{1} \mathcal{T}_k \mathcal{T}_3\right]_{\mathcal{C}} = \begin{pmatrix} 0 & t_{n_1,n_2} & 0 & 0 & \dots & 0 \\ 0 & 0 & t_{n_1+q_2,n_1-q_1} & 0 & \dots & 0 \\ 0 & 0 & 0 & t_{n_1+2q_2,n_1-2q_1} & \dots & 0 \\ \vdots & \vdots & \vdots & \vdots & \dots & \vdots \\ t_{n_1+(P-1)q_2,n_2-(P-1)q_1} & 0 & 0 & 0 & \dots & 0 \end{pmatrix}. \tag{51}$$

The full momentum space will be split into several such $P \times P$ blocks. If we choose another (n_1, n_2) that occurs in the above block as the initial points of the cycle, it will only permute the entries of the block and it will not change the determinant. Thus the full determinant of $\mathcal{H}$ factorizes into cycles with the factor from each cycle being

$$[\det \mathcal{H}]_{\mathcal{C}} = \det\left[1 - \prod_{r=0}^{P-1} t_{n_1-rq_2,n_2+rq_1}\right], \tag{52}$$

which after cyclic permutation of the product of matrices becomes

$$[\det \mathcal{H}]_{\mathcal{C}} = \det\left[1 - \prod_{k=0}^{\beta P} \mathcal{T}\left(n_1 - q_2\frac{k}{\beta}, n_2 + q_1\frac{k}{\beta}\right)\right]. \tag{53}$$

Since products of $\mathcal{T}$ have a unit determinant, it follows that

$$[\det \mathcal{H}]_{\mathcal{C}} = (1-\rho)\left(1 - \frac{1}{\rho}\right), \tag{54}$$

where ρ is the complex eigenvalue of the product of $\mathcal{T}$ around a cycle. The eigenvalues ξ of the full transfer matrix are the Pth roots of ρ and $1/\rho$ in all the cycles. The complex number ρ characterizes the propagation along a cycle. We will show that there are *real* cycles where ρ is either real or a complex number with unit magnitude. If the eigenvalue in the real cycle switches sign as a function of mass, then it will be associated with a nonzero contribution to the parity-even part of Γ.

The product of $\mathcal{T}$ taken along a cycle $\mathcal{C}$ on the two-dimensional momentum torus has the following interpretation. We start with some point $(\frac{n_1}{L}, \frac{n_2}{L})$ on the continuum momentum torus of size 1×1. We move continuously along the direction $(-q_2, q_1)$ and compute the fermion propagation along a closed loop in this direction. One can formally convert this into an interpretation in the continuum without worrying about regularization. The integer momenta (n_1, n_2) cover the entire range of integers in the continuum. The continuum Hamiltonian in the τ direction at a fixed (n_1, n_2) is

$$\tilde{H}(\tau) = -\sigma_2 \frac{2\pi}{l}(n_1 - q_2\tau t) + \sigma_1 \frac{2\pi}{l}(n_2 + q_1\tau t) + \sigma_3 m. \tag{55}$$

We define fermion propagation as

$$\tilde{\phi}(\tau + d\tau) = e^{\tilde{H}(\tau)d\tau}\tilde{\phi}(\tau), \tag{56}$$

in the limit of $d\tau \to 0$. Let $\tilde{\phi}^{\pm}(\infty)$ be the result of propagation from the vector $(1,0)^t$ and $(0,1)^t$ respectively at $\tau = -\infty$. Then,

$$[\det \mathcal{H}]_{\mathcal{C}} = \det\left[1 - \tilde{\phi}^{+}(\infty) \quad \tilde{\phi}^{-}(\infty)\right] \tag{57}$$

in the continuum.

In order to classify cycles, consider the momenta (n_1, n_2) and $(L - n_1, L - n_2)$. From the expression for $\mathcal{T}$ in Eq. (38),

$$\mathcal{T}\left(L - n_1 - q_2\frac{k}{\beta}, L - n_2 + q_1\frac{k}{\beta}\right) = \sigma_3 \mathcal{T}\left(n_1 + q_2\frac{k}{\beta}, n_2 - q_1\frac{k}{\beta}\right)\sigma_3. \tag{58}$$

Using this identity, we now show that if ρ is associated with the (n_1, n_2) cycle, ρ^* is associated with the $(L - n_1, L - n_2)$ cycle. Inserting σ_3^2 between the $\mathcal{T}$'s in Eq. (53), we have

$$\det\left[1 - \prod_{k=0}^{\beta P} \mathcal{T}\left(L - n_1 - q_2\frac{k}{\beta}, L - n_2 + q_1\frac{k}{\beta}\right)\right] = \det\left[1 - \prod_{k=0}^{\beta P} \mathcal{T}\left(n_1 + q_2\frac{k}{\beta}, n_2 - q_1\frac{k}{\beta}\right)\right]. \tag{59}$$

If we take the complex conjugate of the right-hand side, then the product becomes a product of $\mathcal{T}^\dagger$ with the ordering reversed. Using the fact that $\mathcal{T}$'s are Hermitian, and after changing the variable k to $\beta P - k$ so as to recover the original ordering (modulo L), we obtain

$$\det\left[1-\prod_{k=0}^{\beta P}\mathcal{T}\left(L-n_1-q_2\frac{k}{\beta}, L-n_2+q_1\frac{k}{\beta}\right)\right] = \left\{\det\left[1-\prod_{k=0}^{\beta P}\mathcal{T}\left(n_1-q_2\frac{k}{\beta}, n_2+q_1\frac{k}{\beta}\right)\right]\right\}^*. \quad (60)$$

This completes the proof.

We classify cycles in the following way. The cycles $\mathcal{C}$ and $\mathcal{C}^*$ are conjugate if (n_1, n_2) and $(L-n_1, L-n_2)$ belong to $\mathcal{C}$ and $\mathcal{C}^*$ respectively. If $\mathcal{C}$ and $\mathcal{C}^*$ are the same cycle, then we call it a real cycle and denote it by $\mathcal{R}$. If the cycle is real then we have

$$[\det\mathcal{H}]_{\mathcal{R}} = (1-\rho)\left(1-\frac{1}{\rho}\right) = (1-\rho^*)\left(1-\frac{1}{\rho^*}\right). \quad (61)$$

This implies that either ρ is real or ρ is a complex number with unit magnitude. Since the eigenvalues of conjugate cycles are related by complex conjugation, they can be paired together to give a positive contribution to $\det\mathcal{H}$. Therefore, only the real cycles contribute to the phase, which can only be ± 1. The following cases are possible for the real cycles.

(1) When $\rho = e^{i\phi}$, the factor will be real and positive in the above product.
(2) When ρ is real and negative, the contribution will be positive.
(3) When ρ is real and positive, the contribution will be negative.

Depending on the number of real cycles in the above categories, the phase could be either $+1$ or -1. Let us start by assuming that q_1 and q_2 are coprimes. All the cycles have the same length, P, which is even for even L. Let us assume that (n_1, n_2) belongs to a real cycle. Since $(L-n_1, L-n_2)$ belongs to the same cycle, it follows that

$$(L-n_1, L-n_2) = (n_1 - rq_2, n_2 + rq_1) + (k_1 L, k_2 L), \quad (62)$$

for some integers r, k_1 and k_2. Since q_1 and q_2 are coprimes and L is assumed to be even, it follows that r is even and

$$\left(n_1 - \frac{r}{2}q_2, n_2 + \frac{r}{2}q_1\right) = \left((1-k_1)\frac{L}{2}, (1-k_2)\frac{L}{2}\right). \quad (63)$$

Therefore, real cycles have to contain $(n_1, n_2) = (0, 0)$, $(\frac{L}{2}, 0)$, $(0, \frac{L}{2})$ or $(\frac{L}{2}, \frac{L}{2})$. Let $\mathcal{R}_0$ denote the cycle that contains $(n_1, n_2) = (0, 0)$. For every $(-rq_2, rq_1)$ in this cycle there is a partner $(rq_2, -rq_1)$ in the cycle. Only (0, 0), $(\frac{L}{2}, 0)$, $(0, \frac{L}{2})$ or $(\frac{L}{2}, \frac{L}{2})$ have themselves as partners. Since each cycle has an even number of points, we conclude that one of $(\frac{L}{2}, 0)$, $(0, \frac{L}{2})$ or $(\frac{L}{2}, \frac{L}{2})$ also belongs to $\mathcal{R}_0$. Since the length P can have only one factor of 2, the number of cycles, $\frac{L^2}{P}$ has to be even. Since the complex cycles pair up, the two left over from $(\frac{L}{2}, 0)$, $(0, \frac{L}{2})$ and $(\frac{L}{2}, \frac{L}{2})$ have to pair up and belong to another real cycle, which we call $\mathcal{R}_\pi$. If q_1 and q_2 have a common factor, then we will assume that we choose a set of L's that all have this factor while taking the continuum limit. Under such a choice, the common factor of q_1, q_2 and L can be pulled out resulting in multiple cycles traced using coprime steps q_1 and q_2 on a smaller spatial lattice. For the sake of clarity, we demonstrate the above statement in Fig. 2, for the case $q_1 = q_2 = 3$ on a 6^3 lattice.

We now numerically show that the phase for $\mathcal{R}_0$ is 0 and $\mathcal{R}_\pi$ is π for all values of q_1 and q_2 that are coprime. This enables us to write the continuum formula for the phase for this case as

$$\Gamma_{\text{even}} = \pi(q_1 + q_2 + q_1 q_2), \quad (64)$$

in accordance with Eq. (15). In order to maintain numerical stability in the computation of the product of transfer

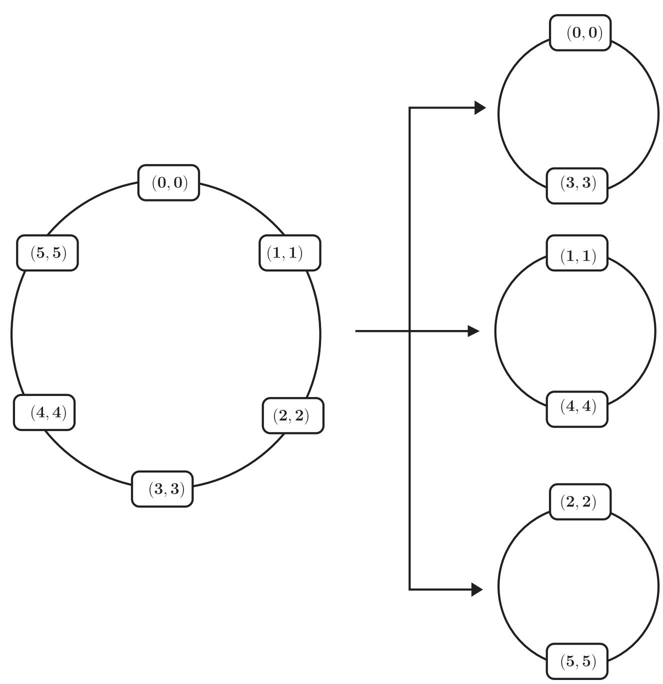

FIG. 2. On the left is the real cycle $\mathcal{R}_0$ with coprime steps $q_1 = q_2 = 1$ on a 6^3 lattice. This cycle has a length $P = 6$. When $q_1 = q_2 = 3$, the cycle $\mathcal{R}_0$ splits into three cycles each of length $P = 2$.

matrices in Eq. (53), we found it useful to normalize each row separately as we multiply and cumulate the normalization factors in a single diagonal matrix. Using this procedure we were able to work with large L and β, thereby essentially seeing the behavior of cycles in the continuum limit. The top left panel in Fig. 3 shows the flow of the phase from each cycle as a function of mass when the background electric flux is $q_1 = 2$ and $q_2 = 3$. The flow is close to what one would see in the continuum since the computations are on a 160^3 lattice. The phase from the real cycle $\mathcal{R}_0$ changes from being π for $m < m_c(L)$ to 0 for $m > m_c(L)$ for some positive $m_c(L)$, which becomes zero in the continuum limit as shown in the top right panel of Fig. 3. The real cycle $\mathcal{R}_\pi$ has a phase of π for all masses. The rest of the cycles are complex and come in pairs as is evident from the plot. The combined phase is only due to the real cycles and is π for all masses above $m_c(L)$. This is consistent with Eq. (64).

It is interesting to focus on the crossing that occurs in the $\mathcal{R}_0$ cycle. In order to zoom in on the crossing, it is better to work on a coarse lattice and we picked $q_1 = 1$ and $q_2 = 0$ on a 4^3 lattice and considered $m \in [0.188138, 0.188144]$. We look at the eigenvalue pair $(\rho, \frac{1}{\rho})$ as the mass is changed in this very small range. The flow of eigenvalues on the complex plane is shown in the bottom panel of Fig. 3. The eigenvalue pair starts out being positive on the low end of the mass region and approaches unity at some m_c which lies within the range. For a range of m above m_c, ρ and $\frac{1}{\rho}$ trace a $|\rho| = 1$ locus on the complex plane. Finally, the ρ becomes real and less than zero. The background with $q_1 = 1$ and the one with $q_3 = 1$ are related by a rotation.

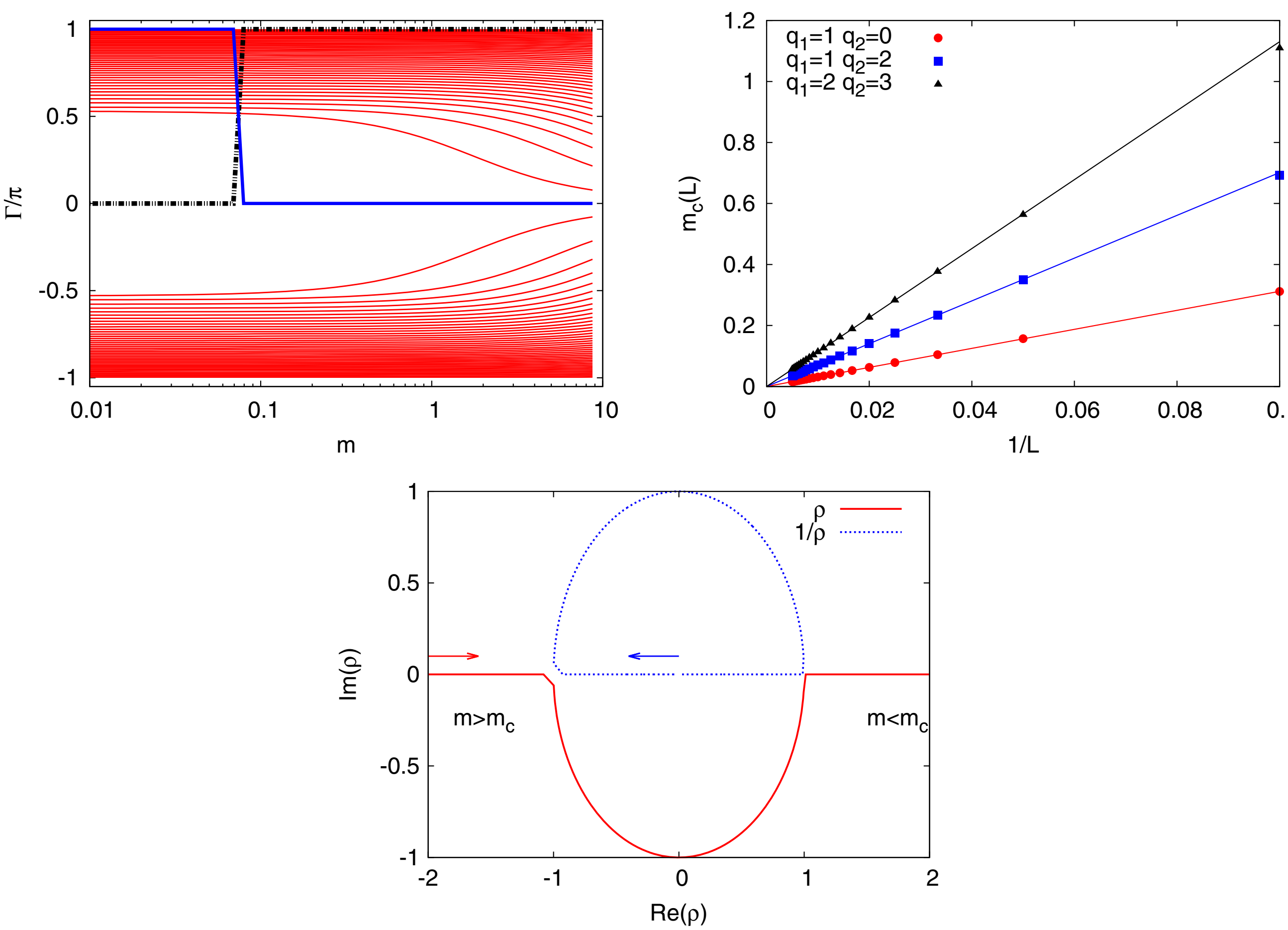

FIG. 3 (color online). The flow of phase from each cycle as a function of mass for a background with fixed electric flux. Top left panel: The flow for all cycles with $q_1 = 2$, $q_2 = 3$ on a 160^3 lattice is shown as red lines. The real cycle $\mathcal{R}_0$ is shown by the solid blue line. In addition the plot shows the overall phase as a black dotted line. It is obvious through a visual inspection that the eigenvalues occur as complex conjugate pairs. The phase of the real cycle, and hence the overall phase, jump at an m_c (the points are only connected to aid the eye). Top right panel: The lattice spacing dependence of m_c is shown for various values of q_1 and q_2. In the continuum limit, $L \to \infty$, the m_c vanishes. Bottom panel: Flow of eigenvalues of the real cycle seen on the complex plane, in the region of crossing around m_c. The plot corresponds to flux $q_1 = 1$, $q_2 = 0$ on a 4^3 lattice in the region $0.188138 < m < 0.188144$. The pair of eigenvalues $(\rho, \frac{1}{\rho})$ flow from real negative values for $m > m_c$ to a complex pair of unit magnitude, and finally to real positive values.

Thus, the zero crossing of an eigenvalue λ^+ in the latter case can now be equivalently understood as the flip in the sign of ρ of the cycle containing the zero mode. The range of m where this behavior occurs shrinks dramatically as one approaches the continuum and the value of m_c gets closer to zero.

As explained, when q_1 and q_2 are not coprimes, the cycles split into N cycles each, ($N = 3$ in the example shown in Fig. 2) depending on the values of q_1 and q_2. Thus, all the N cycles originating from $\mathcal{R}_0$ result in a phase that switches from π to zero as m crosses m_c from below. The other N cycles originating from $\mathcal{R}_\pi$ always have a phase of π. Thus, the total phase becomes

$$\Gamma = \pi(N \mathrm{mod} 2). \tag{65}$$

Only when both q_1 and q_2 are even, N can be even. Thus the expression for the phase remains as Eq. (64) even when q_1 and q_2 are not coprime.

Now we proceed to add h_1 and h_2 to the gauge-field background in Eq. (47). The effect is to replace n_i by $n_i + h_i$ in Eq. (53):

$$[\det \mathcal{H}]_{\mathcal{C}} = \det\left[1 - \prod_{k=0}^{\beta P} \mathcal{T}\left(n_1 + h_1 - q_2\frac{k}{\beta}, n_2 + h_2 + q_1\frac{k}{\beta}\right)\right]. \tag{66}$$

The full determinant still factorizes into cycles but the real cycles now become complex and the previous complex cycles that were complex conjugate pairs are no longer paired. If h_1 and h_2 are multiples of q_2/β and q_1/β respectively, then it is possible to find an integer $k' = k - \frac{\beta h_1}{q_2}$, such that the determinant becomes

$$[\det \mathcal{H}]_{\mathcal{C}} = \det\left[1 - \prod_{k'=0}^{\beta P} \mathcal{T}\left(n_1 - q_2\frac{k'}{\beta}, n_2 + \frac{h_1 q_1 + h_2 q_2}{q_2} + q_1\frac{k'}{\beta}\right)\right]. \tag{67}$$

This means that at any fermion mass and temperature, the phase can only be a function of $h_1 q_1 + h_2 q_2$. In the continuum limit, the fact that we chose a rational h_1 and h_2 should not matter. We proceed to compute the phase per cycle and the total parity-odd part of the phase of the determinant numerically in order to understand the term in the phase that couples h_i with q_i. The two sample cases studied are plotted in Fig. 4. Consider the case of $q_1 = 1$ and $q_2 = 0$ with $h_1 = 0.23$ and $h_2 = 0$ shown in the left panel of Fig. 4. This is just a rotated version of the case with constant magnetic flux and a temporal toron. After removing a factor of -1 from the determinant due to the parity-even part of the phase, the parity-odd part of the phase at the largest mass is consistent with $-2\pi h_1 q_1$ as expected from Eq. (45). Next, we consider the more interesting case of $q_1 = 2$, $q_2 = 3$ with $h_1 = 0.37$ and $h_2 = 0.23$ shown in the right panel of Fig. 4. The parity-even part of the phase is again π as in the previous case. The parity-odd part of the phase at the largest mass is consistent with

$$\Gamma = -2\pi(h_1 q_1 + h_2 q_2), \tag{68}$$

which is indicated by arrows in the plots.

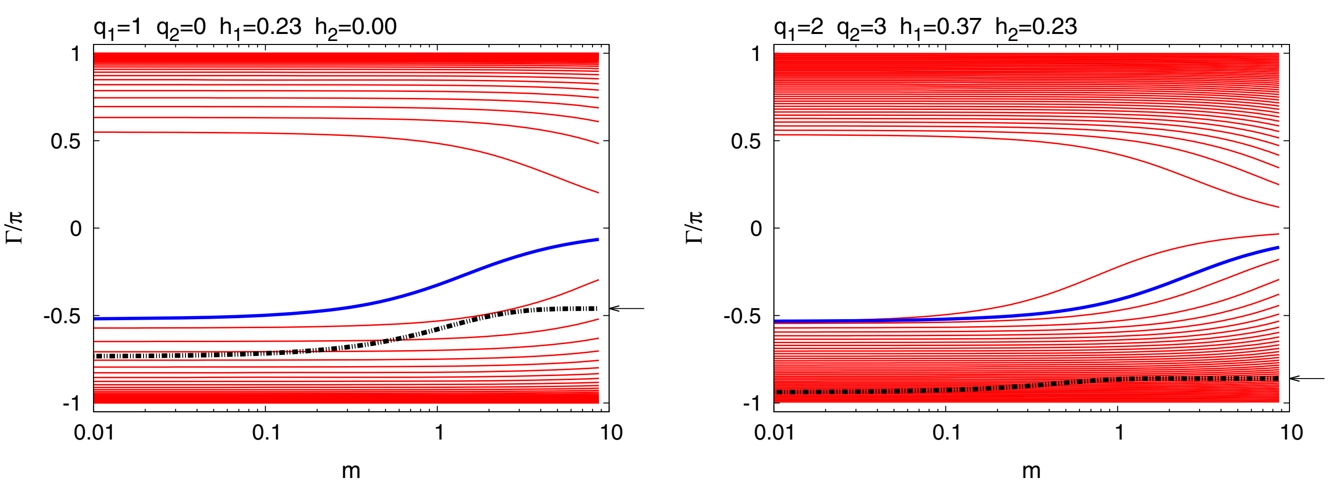

FIG. 4 (color online). The flow of phase from all the cycles (red lines) as a function of mass on a background with fixed electric fluxes and torons. The left panel shows this flow for a background with flux $q_1 = 1$, $q_2 = 0$ and torons $h_1 = 0.23$, $h_2 = 0$ on a 160^3 lattice. Similarly, the right panel is for a background with flux $q_1 = 2$, $q_2 = 3$ and torons $h_1 = 0.37$, $h_2 = 0.23$. The cycle that would have been the real cycle $\mathcal{R}_0$ when torons are absent is specially shown by the solid blue line. The overall parity-odd part of the phase is shown as the black dashed line. The arrows indicate the expectations from Eq. (68) for the infinite mass limit.

C. Uniform and static electric and magnetic fields

Now we consider the gauge-field background where electric as well as magnetic fields are present i.e., q_1, q_2 and q_3 terms are all present in Eq. (20) with no torons. We are unable to study this case analytically. Therefore, we study this general case by directly evaluating Eq. (32). We check for any loss of precision by comparing the determinant of the product of $\mathcal{T}_k$ to 1. Doing so, we were able to use up to 12^3 lattices. We find that $\det D$ is real for any q_1, q_2 and q_3. Thus, the phase can only be ± 1 and its expression must be of the form

$$\Gamma = \eta_1 \pi (q_1 + q_2 + q_3) + \eta_2 \pi (q_1 q_2 + q_2 q_3 + q_3 q_1) + \eta_3 \pi q_1 q_2 q_3, \tag{69}$$

where $\eta_i = 0$ or 1. Rotational symmetry guarantees that each η_i is the same for all directions. From the last section, we know that $\eta_1 = \eta_2 = 1$. We do not have any analytical argument about η_3. In Table I, we collect our observations about the dependence of phase on q_1, q_2 and q_3. The results of the table are robust and found to be the same on $L = 4$, 6, 8, 10 and 12 lattices, and for various even and odd values for the q's. The entries with $q_3 = 0$ reiterate our observations of the last subsection. The entry with even q_1 and q_2 includes the case $q_1 = q_2 = 0$, which we understand as due to the mismatch between the number of positive and negative eigenvalues of a two-dimensional Dirac operator. The other cases do not offer a simple analytical explanation. The important entry is the last one where all q's are odd. Since the phase is even, it implies that $\eta_3 = 0$. Thus, $\det D$ has a parity-even phase given by

$$\Gamma = \pi (q_1 + q_2 + q_3) + \pi (q_1 q_2 + q_2 q_3 + q_3 q_1). \tag{70}$$

V. PERTURBATION THEORY: PARITY-ODD CONTRIBUTIONS

In this section, we return to the case of a uniform and static magnetic field in the presence of a uniform toron in the Euclidean time direction that was studied in Sec. IV A and consider perturbations A_1^p and A_2^p on this background. We expand the determinant for $\mathcal{H}$ in Eq. (32) in powers of A_i^p while considering the constant flux background and the toron to be nonperturbative. The transfer matrix $\mathcal{T}_k$ can be expanded to second order in A_i^p as

$$\mathcal{T}_k = \mathcal{T} + \mathcal{F}_k + \mathcal{S}_k. \tag{71}$$

The detailed expressions for $\mathcal{F}_k$ and $\mathcal{S}_k$ are given in Appendix A. We write

$$\prod_{k=\beta}^{1} \mathcal{T}_k = \mathcal{T}^\beta [1 + P], \tag{72}$$

where

$$P = \sum_{k=0}^{\beta-1} \mathcal{T}^{-k-1} \mathcal{F}_{k+1} \mathcal{T}^k + \sum_{k=0}^{\beta-1} \mathcal{T}^{-k-1} \mathcal{S}_{k+1} \mathcal{T}^k + \sum_{k=1}^{\beta-1} \sum_{l=0}^{k-1} \mathcal{T}^{-k-1} \mathcal{F}_{k+1} \mathcal{T}^{k-l-1} \mathcal{F}_{l+1} \mathcal{T}^l. \tag{73}$$

From Eq. (32), we have

$$\log \det \mathcal{H} = \log \det \mathcal{H}_{\rm st} + \log \det \left[1 + \mathcal{H}_{\rm st}^{-1} P T_3^\dagger\right]. \tag{74}$$

Using standard perturbation theory in the eigenbasis of the unperturbed $\mathcal{T}$, we arrive at

$$\begin{aligned} \log \det \left[1 + \mathcal{H}_{\rm st}^{-1} P T_3^\dagger\right] = {} & \sum_{i\pm} \sum_{k=0}^{\beta-1} \frac{e^{\pm(\beta-1)\lambda_i^\pm - i2\pi h_3}}{1 + e^{\pm\beta\lambda_i^\pm - i2\pi h_3}} \mathcal{F}_{k+1}^{i\pm,i\pm} + \sum_{i\pm} \sum_{k=0}^{\beta-1} \frac{e^{\pm(\beta-1)\lambda_i^\pm - i2\pi h_3}}{1 + e^{\pm\beta\lambda_i^\pm - i2\pi h_3}} \mathcal{S}_{k+1}^{i\pm,i\pm} \\ & - \frac{1}{2} \sum_{i\pm} \sum_{j\pm} \sum_{k=0}^{\beta-1} \frac{e^{\pm(\beta-1)\lambda_i^\pm \pm(\beta-1)\lambda_j^\pm - i4\pi h_3}}{(1 + e^{\pm\beta\lambda_i^\pm - i2\pi h_3})(1 + e^{\pm\beta\lambda_j^\pm - i2\pi h_3})} \mathcal{F}_{k+1}^{i\pm,j\pm} \mathcal{F}_{k+1}^{j\pm,i\pm} \\ & + \sum_{i\pm} \sum_{j\pm} \sum_{k=1}^{\beta-1} \sum_{l=0}^{k-1} \frac{e^{\pm(\beta-k+l-1)\lambda_i^\pm \pm(k-l-1)\lambda_j^\pm - i2\pi h_3}}{(1 + e^{\pm\beta\lambda_i^\pm - i2\pi h_3})(1 + e^{\pm\beta\lambda_j^\pm - i2\pi h_3})} \mathcal{F}_{k+1}^{i\pm,j\pm} \mathcal{F}_{l+1}^{j\pm,i\pm} + \mathcal{O}(A^3), \end{aligned} \tag{75}$$

where it is implicit that the summation over $i+$ runs up to $V + q_3$, while that of $i-$ up to $V - q_3$. We use this general second order perturbative expression to study two cases of interest.

A. Zero temperature

We assume that we are working away from the massless limit and therefore $\lim_{L\to\infty} L\lambda_i^\pm$ is strictly greater than zero for all i. Since $\beta = \frac{L}{t}$, we see that in the limit $t \to 0$, the first

TABLE I. Phase Γ for various combinations of q_1, q_2 and q_3. The "0" represents even integers and "1" represents odd integers.

q_1	q_2	q_3	Γ/π
0	0	0	0
0	0	1	1
0	1	0	1
0	1	1	1
1	0	0	1
1	0	1	1
1	1	0	1
1	1	1	0

three terms in Eq. (75) are real and do not contribute to the phase. The last term can be simplified as follows. Let

$$|\mathcal{F}^{i\pm,j\pm}_{k+1}\mathcal{F}^{j\pm,i\pm}_{l+1}| < X^{i\pm,j\pm}, \tag{76}$$

where the upper bound $X^{i\pm,j\pm}$ is independent of β. Then, the sum is bounded above by

$$\begin{aligned} &Y_{i\pm,j\pm}(\beta) \\ &= \frac{e^{\pm(\beta-1)\lambda_i^\pm - i2\pi h_3}}{1+e^{\pm\beta\lambda_i^\pm - i2\pi h_3}} \\ &\times \frac{1}{1+e^{\pm\beta\lambda_j^\pm - i2\pi h_3}} \frac{\beta(1-e^{\pm\lambda_j^\pm \mp\lambda_i^\pm}) + (1-e^{\beta(\pm\lambda_j^\pm\mp\lambda_i^\pm)})}{2(\cosh(\pm\lambda_j^\pm \pm\lambda_i^\pm)-1)} X^{i\pm,j\pm}. \end{aligned} \tag{77}$$

Explicitly, $Y_{i+,j+}$ and $Y_{i-,j-}$ vanish in the $\beta\to\infty$ limit. Therefore, we need to consider only the products of $\mathcal{F}^{i+,j-}_{k+1}$ and $\mathcal{F}^{i-,j+}_{l+1}$ terms. The phase is

$$\begin{aligned} \Gamma = \pi q_3 - 2\pi h_3 q_3 + \lim_{\beta\to\infty} \sum_{i=1}^{V+q_3}\sum_{j=1}^{V-q_3} e^{(\lambda_j^- - \lambda_i^+)} \\ \times \sum_{k=1}^{\beta-1}\sum_{l=0}^{k-1}(e^{(l-k)(\lambda_i^+ + \lambda_j^-)} - e^{(k-l-\beta)(\lambda_i^+ + \lambda_j^-)}) \\ \times \mathrm{Im}\mathcal{F}^{i+,j-}_{k+1}\mathcal{F}^{j-,i+}_{l+1}. \end{aligned} \tag{78}$$

The second term does not depend on h_3 and therefore the contribution from the toron h_3 and the perturbative part are independent of each other at this order. If we assume $\frac{k-l}{L}$ is kept finite in the infinite L limit, then we can ignore the second factor in the parentheses of the second term. The term $2\pi q_3 h_3$ is independent of m and changes in multiples of 2π under large gauge transformation $h_3 \to h_3 + 1$. Even at zero temperature, the induced gauge action is not of the type in Eq. (2) if we include fields that do not vanish at infinity.

B. Finite temperature and $h_3 = 0$

Our aim in this subsection is to study the purely perturbative contribution to the phase in a possibly nonperturbative background at finite temperature. Since we are focusing on terms of the type $A_1^p A_2^p$, we set $h_3 = 0$. In addition we only consider $A_1^p(k)$ and $A_2^p(k)$ that depend only on time. When $h_3 = 0$, the first three terms in Eq. (75) are real even at finite β. The phase becomes

$$\Gamma = \sum_{i\pm}\sum_{j\pm}\sum_{k=1}^{\beta-1}\sum_{l=0}^{k-1}\frac{e^{\pm(\beta-k+l-1)\lambda_i^\pm \pm(k-l-1)\lambda_j^\pm}}{(1+e^{\pm\beta\lambda_i^\pm})(1+e^{\pm\beta\lambda_j^\pm})}\mathrm{Im}\mathcal{F}^{i\pm,j\pm}_{k+1}\mathcal{F}^{j\pm,i\pm}_{l+1}. \tag{79}$$

After writing

$$\mathcal{F}^{i\pm,j\pm}_k = \sum_{\mu=1}^{2}\tilde{\mathcal{F}}^{i\pm,j\pm}_\mu A^p_\mu(k), \tag{80}$$

we arrive at an expression for the phase, which is written concisely as

$$\Gamma = -\sum_{k=1}^{\beta-1}\sum_{l=0}^{k-1} G(k-l)[A_1^p(k)A_2^p(l) - A_2^p(k)A_1^p(l)]. \tag{81}$$

The form factor G is

$$\begin{aligned} G(k) = \sum_{(i\pm,j\pm)} e^{\mp\lambda_i^\pm \mp\lambda_j^\pm}\frac{\sinh[(\frac{\beta}{2}-k)(\pm\lambda_i^\pm \mp\lambda_j^\pm)]}{4\cosh\frac{\beta\lambda_i^\pm}{2}\cosh\frac{\beta\lambda_j^\pm}{2}} \\ \times \mathrm{Im}[(\tilde{\mathcal{F}}^{i\pm,j\pm}_1)^*\tilde{\mathcal{F}}^{i\pm,j\pm}_2]. \end{aligned} \tag{82}$$

It satisfies the antisymmetric property

$$G(\beta-k) = -G(k). \tag{83}$$

This expression is valid for all q_3, h_1 and h_2. For the free case $q_3 = 0$ that we discussed in Sec. III A, the form factor simplifies to

$$G(k) = \sum_p \frac{\sinh[(\beta-2k)\lambda_p]}{2\cosh^2\frac{\beta\lambda_p}{2}}\mathrm{Im}[(\tilde{\mathcal{F}}^{p+,p-}_1)^*\tilde{\mathcal{F}}^{p+,p-}_2]. \tag{84}$$

We derive the expressions for $\mathcal{F}^{p+,p-}_\mu$ in Appendix B.

The behavior of this form factor G is shown as a function of time $\tau = \frac{k}{L}$ in Fig. 5. The observations about the long- and short-distance behavior of $G(\tau)$ seen in the two panels of the figure can be summarized in the following way. The $G(\tau)$ has a leading $\frac{1}{L}$ lattice correction. However, the coefficient of $\frac{1}{L}$ shows a singular τ^{-3} behavior. That is, the approach to the continuum limit is given by

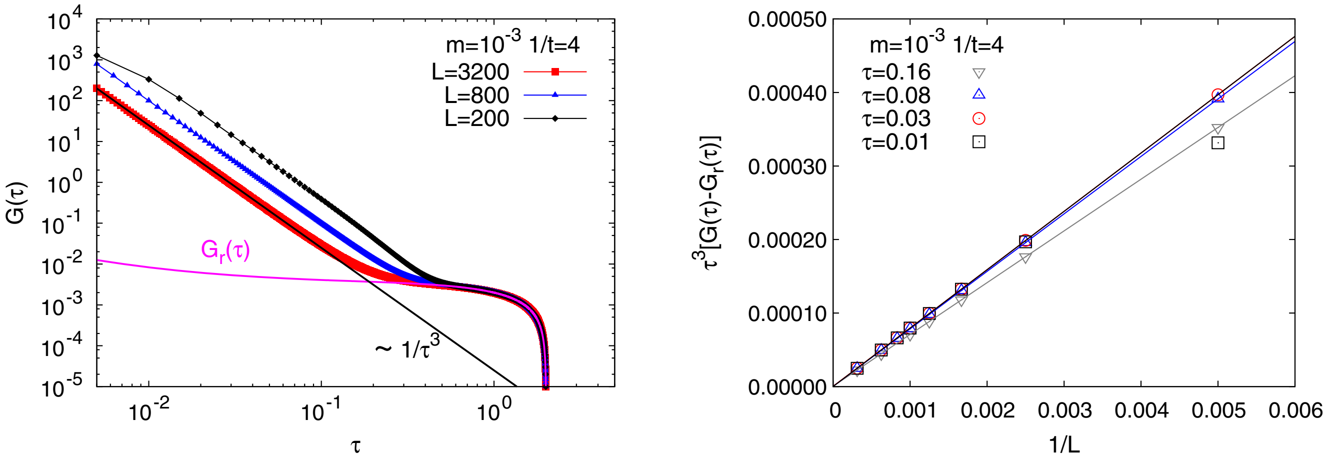

FIG. 5 (color online). Left panel: The form factor $G(\tau)$ at fermion mass $m = 10^{-3}$ is shown at a temperature $t = 0.25$ for the free $q_3 = 0$ background gauge field with no torons. The different symbols correspond to different L's. At all L's, $G(\tau)$ shows a τ^{-3} behavior at small values of τ. The best fit for this power law τ^{-3} using the $L = 3200$ data is shown as the black straight line. When the continuum is approached by increasing L, the power-law behavior shifts to the left on the log-log plot such that $G(\tau)$ approaches $G_r(\tau)$ [refer to Eq. (87)] at all τ's. This continuum limit $G_r(\tau)$ is shown as the magenta curve. Right panel: The approach to continuum of the scaled variable $\tau^3[G(\tau) - G_r(\tau)]$ is shown at various τ's. At all τ's, it approaches 0 with a dominant $\frac{1}{L}$ scaling. For very small τ, there is data collapse suggesting a perfect τ^{-3} scaling. At larger τ, there are corrections to this scaling. However, it is the most singular τ^{-3}/L behavior of $G(\tau)$ that is important to the phase of $\det D$.

$$G(\tau L) = G_r(\tau) + \frac{1}{L} G_s(\tau) + \mathcal{O}\left(\frac{1}{L^2}\right), \tag{85}$$

where $G_r(\tau)$ is the continuum limit, while the singular coefficient of the dominant $\frac{1}{L}$ correction is given by

$$G_s(\tau) = \frac{f(m,t)}{\tau^3} + \mathcal{O}(\tau^{-2}), \tag{86}$$

for some mass- and temperature-dependent function f. The continuum limit $G_r(\tau)$ seems to be well described by the regulator-independent limit obtained by replacing $\lambda_p L$ by its $p \approx 0$ limit, Λ_p i.e.,

$$G_r(\tau) = \sum_n \frac{m}{\Lambda_n} \frac{\sinh[(\frac{1}{t} - 2\tau)\Lambda_n]}{2\cosh^2[\frac{\Lambda_n}{2t}]}, \tag{87}$$

making use of

$$\Lambda_n \equiv \lim_{L\to\infty} L\lambda_p = \sqrt{m^2 + 4\pi^2(n_1^2 + n_2^2)}$$
$$\text{and} \quad \lim_{L\to\infty} \mathrm{Im}[(\tilde{\mathcal{F}}_1^{p+,p-})^* \tilde{\mathcal{F}}_2^{p+,p-}] = \frac{m}{\Lambda_n}, \tag{88}$$

for all momenta even though they only hold true for $p_i \approx 0$. The above observations about G are seen at all mass and temperature.

Let us consider the following perturbative fields chosen such that there is a nonzero Chern-Simons action:

$$A_1^p(k) = \frac{c}{L} \sin\left(\frac{2\pi n_3 k}{\beta}\right)$$
$$\text{and} \quad A_2^p(k) = \frac{c}{L} \cos\left(\frac{2\pi n_3 k}{\beta}\right). \tag{89}$$

The phase becomes

$$-\frac{\Gamma}{c^2} = \lim_{L\to\infty} \frac{1}{L^2} \sum_{k=1}^{\beta-1} (\beta - k) G(k) \sin\left(\frac{2\pi n_3 k}{\beta}\right)$$
$$= \lim_{L\to\infty} \frac{\beta}{L^2} \sum_{k=1}^{\frac{\beta}{2}} G(k) \sin\left(\frac{2\pi n_3 k}{\beta}\right), \tag{90}$$

where we have made a change of variable from k and l to $k - l$, and used the antisymmetry property of $G(k)$ in Eq. (83). Inserting Eq. (85) for $G(k)$, we obtain

$$-\frac{\Gamma}{c^2} = \lim_{L\to\infty} \frac{\beta}{L^2} \sum_{k=1}^{\beta-1} G_r(k) \sin\left(\frac{2\pi n_3 k}{\beta}\right)$$
$$+ \lim_{L\to\infty} \beta \sum_{k=1}^{\frac{\beta}{2}} \frac{f(m,t)}{k^3} \sin\left(\frac{2\pi n_3 k}{\beta}\right). \tag{91}$$

The first term arising from the continuum part of $G(\tau)$ can be converted to an integral. The second term that arises from the singular part contributes in the continuum due to the τ^{-3} behavior. The two terms can be expressed as

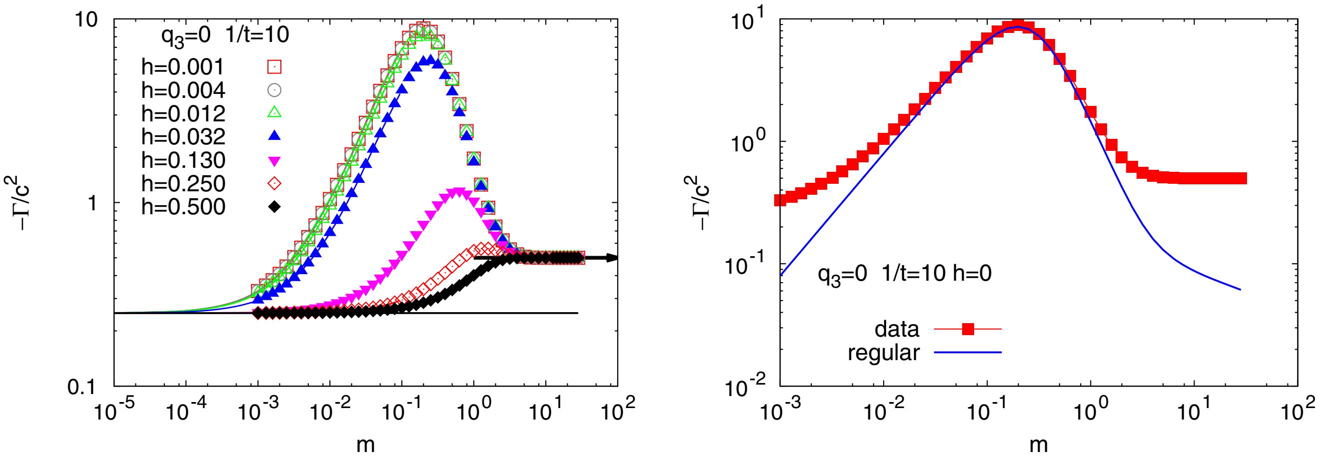

FIG. 6 (color online). The crossover of phase from the $m \to 0$ limit (which is $\Gamma = -\frac{c^2}{4}$) to the $m \to \infty$ limit ($\Gamma = -\frac{c^2}{2}$) when $q_3 = 0$. In the left panel, the mass dependence of Γ is shown for various values of $h_1 = h_2 = h$ specified by different symbols. For large values of mass ($m \gtrsim 10$), the phase is $-\frac{c^2}{2}$. For small values of mass, the phase approaches $-\frac{c^2}{4}$ as seen by extrapolation (solid lines) using data points with $m < 0.1$. In the right panel, the phase Γ (red squares) and the phase calculated only using $G_r(\tau)$ (blue line) are compared when $h = 0$.

$$-\frac{\Gamma}{c^2} = \frac{1}{t}\int_0^{\frac{1}{2t}} G_r(\tau)\sin(2\pi n_3 \tau t)d\tau + 2\pi n_3 f(m,t)\zeta(2). \tag{92}$$

The second term is proportional to the momentum n_3 and hence it is indeed the local Chern-Simons term. It contributes both in the infinite mass and massless limit showing that the parity-odd contribution is regulator dependent [4,13]. At very low but nonzero temperatures, the contribution from the first term behaves as

$$\frac{\Gamma_{\rm reg}}{c^2} \approx -\frac{\pi n_3}{2}\sum_{n_1,n_2=0}^{\infty}\frac{m(1-e^{-\frac{2\Lambda_{\tilde{n}}}{t}})}{\Lambda_{\tilde{n}}[\Lambda_{\tilde{n}}^2 + n_3^2\pi^2 t^2]} \quad \text{where } \tilde{n}_i = n_i + h_i, \tag{93}$$

after integration over τ. This right away makes it explicit the dependence of the phase on the torons h_1 and h_2 in the $q_3 = 0$ background. When the torons are absent, this infinite sum suffers from an infrared divergence when the $t \to 0$ limit is taken before the $m \to 0$ limit. But the sum becomes zero when the two limits are interchanged. In the $m \to \infty$ limit, the infinite sum always vanishes. Thus, the phase from the regular term is zero in both the infinite and zero mass limits and only the singular part contributes to the parity-odd phase in these two limits. At any finite and nonzero mass the contribution from the regular term is not local since it is not linear in n_3.

The above discussion shows where the parity-breaking phase arises at different masses. We now present results on the phase directly calculated using Eq. (81). In the left panel of Fig. 6, we show the behavior of the phase as a function of fermion mass, for the perturbation in Eq. (89) on a $q_3 = 0$ background. We show the behavior at various values of $h_1 = h_2 = h$, and at a temperature $t = 0.1$. We did the numerical calculation using lattices with $L = 60$, 80, 100, 120, 140 and 160. With these, we did a continuum extrapolation for Γ using a fourth order polynomial in $\frac{1}{L}$. Changing the order of the polynomial to three or five made little difference to the results. In the figure, we show these continuum extrapolated values. When $m \to \infty$, the phase becomes $-\frac{c^2}{2}$ which is consistent with a Chern-Simons coefficient $\kappa = -1$. Using the values of phase for $m < 0.1$, we extrapolated the results to $m = 0$ using a fourth order polynomial in m. These extrapolations are shown by the solid lines. The extrapolated curves smoothly approach $-\frac{c^2}{4}$ as $m \to 0$, independent of h. This corresponds to a Chern-Simons coefficient $\kappa = -\frac{1}{2}$, which is consistent with [13]. At other intermediate values of m, we find a strong dependence on h_1 and h_2, which is expected from the above discussions for the $q_3 = 0$ case. From the right panel of Fig. 6, it is clear that the toron dependence of the phase indeed comes from $G_r(\tau)$. As t becomes smaller, the peak gets higher and shifts to smaller values of m according to Eq. (93).

In Fig. 7, we show a similar plot for a $q_3 = 1$ background. We do not find any dependence on the spatial torons. Therefore, we show only the result with $h_1 = h_2 = 0$. The different symbols are the continuum extrapolated results at four different temperatures. Using a similar procedure as in the $q_3 = 0$ case, we find the phase to be $-\frac{c^2}{2}$ and $-\frac{c^2}{4}$ in the infinite and zero mass limits respectively. At finite values of m, there is a smooth crossover between the two limits. At smaller t, this crossover occurs at smaller values of m, well described by an $\frac{m}{t}$ dependence of the phase.

The above mass dependence is clearly h_1, h_2 and q_3 dependent. Although implicit, one could consider them as

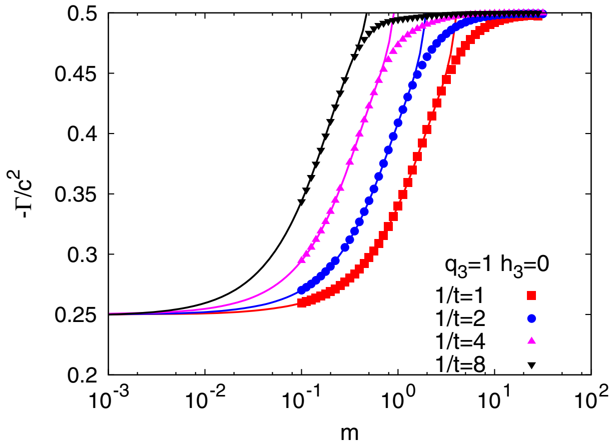

FIG. 7 (color online). The mass dependence of phase Γ with a flux $q_3 = 1$ in the xy plane. The different symbols correspond to various temperatures t which range from 1 to $\frac{1}{8}$. The solid lines show the polynomial extrapolation of the phase from small $m < 0.1$ to $m = 0$. It is seen that the phase approaches $-\frac{1}{2}$ at large mass and the extrapolation shows that the phase approaches $-\frac{1}{4}$ when $m \to 0$.

$h_i - A_i^p$ and $q_3 - A_i^p$ terms in the induced gauge action, that originates from the infrared and would not be predicted by a pure Chern-Simons term.

VI. CONCLUSIONS

We studied the contribution to the phase of the fermion determinant in QED$_3$ using lattice regularization and Wilson fermions at finite volume and temperature. We considered nonperturbative backgrounds that contain nonzero magnetic and electric flux. In addition, our backgrounds also contained constant gauge potentials referred to as torons. In the absence of torons and any perturbation, we studied the parity-even contribution to the phase and our result in Eq. (15) is an extension of the result in [22–24] for the case of just a magnetic flux. In the presence of a toron in the time direction and a nonzero magnetic flux, our result using lattice regularization agreed with one obtained using zeta function regularization [18,19]. We extended this result for the case with electric fluxes and torons. In addition to extending the result, we provided an alternate way of understanding the parity-even contribution when one has a magnetic flux. The connection between two-dimensional topology and a parity-even phase is translated to a sign associated with the propagation of a free fermion along a closed loop in a two-dimensional momentum torus where the momentum associated with the propagation changes as one goes along the closed loop. The direction associated with the closed loop in the two-dimensional momentum torus is proportional to $(-q_2, q_1)$, the fluxes associated with the electric field.

The effect of finite temperature on the coefficient of the induced Chern-Simons term discussed in the past [14] was addressed here. In addition we also addressed the issue of finite mass. We showed that the contribution at zero mass and infinite mass only comes from the regulator but there is also a contribution from the continuum part at nonzero finite masses. Whereas the contribution from the regulator is local and of the Chern-Simons type with a coefficient that is different at zero and infinite mass [13], the contribution at any finite nonzero mass is not local. In addition, the result depends on the presence of torons in the space directions if there is no magnetic flux. This is associated with the eigenvalues of the free two-dimensional Dirac operator depending on the torons and the eigenvalues of the two-dimensional Dirac operator in the presence of a nonzero magnetic flux being independent of the torons [29].

Our studies in various nonperturbative backgrounds suggested that we can study the following class of theories using numerical simulation:

$$Z = \int [DU] \prod_{j=1}^{N^+} [d\psi_j^+][d\bar{\psi}_j^+] \prod_{k=1}^{N^-} [d\psi_k^-][d\bar{\psi}_k^-] e^{S_g(U) + \sum_{j=1}^{N^+} \bar{\psi}_j (\not{D}_n - B + M_k^+)\psi_j \sum_{k=1}^{N^-} \bar{\psi}_j (\not{D}_n + B - M_j^-)\psi_j}, \tag{94}$$

with $0 < M_k^+$ and $M_j^- < 1$. The simplest one to simulate is the one that does not break parity: Set $N^+ = N^- = N$ and $M_k^- = M_k^+ = M$. This theory with N degenerate flavors is expected to have nonzero values for fermion bilinears that do not break parity in the massless limit [6]. It would be interesting to perform a large N analysis on the lattice formalism in addition to performing a numerical simulation at small values of N. Motivated by [30] it would be interesting to study the theory $N^- = 0$, $N^+ = N$ and $M_k^+ = M$. In particular, one could attempt to first study this theory for large N semiclassically using the lattice formalism where the nonperturbative effects modify the induced parity-odd term at finite volume and temperature away from the conventional Chern-Simons term in order to preserve gauge invariance. A numerical study has to address the sign problem which might be under control for large N. Since chiral symmetry is not relevant and gauge invariance is maintained on the lattice with Wilson fermions, numerical studies can be performed with the aim of studying massless fermions without the necessity to use a formalism that preserves chiral symmetry [25,31].

ACKNOWLEDGMENTS

The authors acknowledge partial support by the NSF under Grant No. PHY-1205396.

APPENDIX A: EXPRESSIONS FOR $\mathcal{F}$ AND $\mathcal{S}$

We derive the expressions for perturbative terms $\mathcal{F}$ and $\mathcal{S}$ in Eq. (71). As explained in Sec. V, we consider perturbative fields $A_i^p(k)$ which are only dependent on time k. We expand B_k and C_k to second order in perturbation theory

$$\begin{aligned} B_k &\equiv B + \sum_{i=1}^{2} A_i^p(k)\tilde{b}_i^1 + \sum_{i=1}^{2} A_i^p(k)A_j^p(k)\tilde{b}_i^2, \\ &\equiv B + b_k^1 + b_k^2. \end{aligned} \tag{A1}$$

Similarly for C_k:

$$\begin{aligned} C_k &\equiv C + \sum_{i=1}^{2} A_i^p(k)\tilde{c}_i^1 + \sum_{i=1}^{2} A_i^p(k)A_j^p(k)\tilde{c}_i^2, \\ &\equiv c_k^1 + c_k^2. \end{aligned} \tag{A2}$$

Since only first order terms seem to contribute to the phase, we write down their expressions:

$$\begin{aligned} \tilde{b}_i^1 &= \frac{-i}{2}(T_i - T_i^\dagger), \\ \tilde{c}_1^1 &= \frac{i}{2}(T_1 + T_1^\dagger), \\ \tilde{c}_2^1 &= \frac{1}{2}(T_2 + T_2^\dagger). \end{aligned} \tag{A3}$$

The T_i's are the forward shift operators evaluated on a free or constant magnetic field background. Then, B^{-1} can be expanded to second order as

$$B_k^{-1} = B^{-1} - B^{-1}b_k^1B^{-1} - B^{-1}b_k^2B^{-1} + B^{-1}b_k^1B^{-1}b_k^1B^{-1}. \tag{A4}$$

Using the above expressions, one can trace the steps sketched in Eq. (71) to obtain

$$\begin{aligned} \mathcal{T}_k &= \mathcal{T} + \mathcal{F}_k + \mathcal{S}_k, \\ \mathcal{T} &= \begin{pmatrix} B^{-1} & -B^{-1}C^\dagger \\ -CB^{-1} & CB^{-1}C^\dagger + B \end{pmatrix}, \\ \mathcal{F}_k &= \begin{pmatrix} -B^{-1}b_k^1B^{-1} & -B^{-1}c_k^{1\dagger} + B^{-1}b_k^1B^{-1}C^\dagger \\ -c_k^1B^{-1} + CB^{-1}b_k^1B^{-1} & (b_k^1 + c_k^1B^{-1}C^\dagger \\ & -CB^{-1}b_k^1B^{-1}C^\dagger + CB^{-1}c_k^{1\dagger}) \end{pmatrix}, \\ \mathcal{S}_k &= \begin{pmatrix} -B^{-1}b_k^2B^{-1} + B^{-1}b_k^1B^{-1}b_k^1B^{-1} & (-B^{-1}c_k^{2\dagger} + B^{-1}b_k^1B^{-1}c_k^{1\dagger} \\ & +B^{-1}b_k^2B^{-1}C^\dagger - B^{-1}b_k^1B^{-1}b_k^1B^{-1}C^\dagger) \\ (-c_k^2B^{-1} + c_k^1B^{-1}b_k^1B^{-1} & (b_k^2 + c_k^2B^{-1}C^\dagger - c_k^1B^{-1}b_k^1B^{-1}C^\dagger \\ +CB^{-1}b_k^2B^{-1} - CB^{-1}b_k^1B^{-1}b_k^1B^{-1}) & +CB^{-1}b_k^1B^{-1}b_k^1B^{-1}C^\dagger + c_k^1B^{-1}c_k^{1\dagger} \\ & -CB^{-1}b_k^1B^{-1}c_k^{1\dagger} + CB^{-1}c_k^{2\dagger}) \end{pmatrix}. \end{aligned} \tag{A5}$$

It is straightforward to obtain $\tilde{\mathcal{F}}$ and $\tilde{\mathcal{S}}$ from the above expressions in terms of $\tilde{b}_i^1$ and $\tilde{c}_i^1$.

APPENDIX B: PERTURBATION THEORY IN THE MOMENTUM BASIS

In this appendix, we derive first order terms obtained in Appendix A in the momentum basis. Using the Fourier transforms of Eq. (A3), one obtains

$$\tilde{\mathcal{F}}_i = \begin{pmatrix} \alpha_i & \beta_i \\ \beta_i^* & \gamma_i \end{pmatrix}, \quad \text{where}$$

$$\begin{pmatrix} \alpha_1 & \beta_1 \\ \beta_1^* & \gamma_1 \end{pmatrix} = \begin{pmatrix} -\frac{\sin p_1}{b^2} & \frac{i\cos p_1}{b} + \frac{c^*\sin p_1}{b^2} \\ -\frac{i\cos p_1}{b} + \frac{c\sin p_1}{b^2} & \sin p_1(1-\frac{|c|^2}{b^2}) + \frac{i(c^*-c)\cos p_1}{b} \end{pmatrix},$$

$$\begin{pmatrix} \alpha_2 & \beta_2 \\ \beta_2^* & \gamma_2 \end{pmatrix} = \begin{pmatrix} -\frac{\sin p_2}{b^2} & -\frac{\cos p_2}{b} + \frac{c^*\sin p_2}{b^2} \\ -\frac{\cos p_2}{b} + \frac{c\sin p_2}{b^2} & \sin p_2(1-\frac{|c|^2}{b^2}) + \frac{(c^*+c)\cos p_2}{b} \end{pmatrix}. \tag{B1}$$

Using the expressions for the eigenvalues and eigenvectors of $\mathcal{T}(p)$,

$$\tilde{\mathcal{F}}_i^{p+,p-} = \frac{\alpha_i|c|^2 + \beta_i c^*(1-e^{\lambda_p}b) + \beta_i^* c(1-e^{-\lambda_p}b) + \gamma_i(1+b^2-2b\cosh\lambda_p)}{\sqrt{[|c|^2+(1-e^{\lambda_p}b)^2][|c|^2+(1-e^{-\lambda_p}b)^2]}}, \tag{B2}$$

for any generic mode. For the zero and doubler modes, it is

$$\tilde{\mathcal{F}}_i^{p+,p-} = \begin{cases} \beta_i & \text{if } b<1 \\ \beta_i^* & \text{if } b>1. \end{cases} \tag{B3}$$

When $p \approx 0$, using Eq. (88), we can replace λ_p with Λ_n/L in Eq. (B2) for $\tilde{\mathcal{F}}_1$ and $\tilde{\mathcal{F}}_2$. By expanding $\mathrm{Im}(\tilde{\mathcal{F}}_1^*\tilde{\mathcal{F}}_2)$ as a power series in $1/L$, we obtain the expression

$$\lim_{L\to\infty} \mathrm{Im}[(\tilde{\mathcal{F}}_1^{p+,p-})^* \tilde{\mathcal{F}}_2^{p+,p-}] = \frac{m}{\Lambda_n}. \tag{B4}$$

[1] S. Deser, R. Jackiw, and S. Templeton, Ann. Phys. (N.Y.) **140**, 372 (1982).
[2] S. Deser, R. Jackiw, and S. Templeton, Phys. Rev. Lett. **48**, 975 (1982).
[3] A. Niemi and G. Semenoff, Phys. Rev. Lett. **51**, 2077 (1983).
[4] A. Redlich, Phys. Rev. D **29**, 2366 (1984).
[5] C. Vafa and E. Witten, Commun. Math. Phys. **95**, 257 (1984).
[6] R. D. Pisarski, Phys. Rev. D **29**, 2423 (1984).
[7] J. Braun, H. Gies, L. Janssen, and D. Roscher, Phys. Rev. D **90**, 036002 (2014).
[8] S. Hands, J. Kogut, and C. Strouthos, Nucl. Phys. **B645**, 321 (2002).
[9] S. Hands, J. Kogut, L. Scorzato, and C. Strouthos, Phys. Rev. B **70**, 104501 (2004).
[10] R. Fiore, P. Giudice, D. Giuliano, D. Marmottini, A. Papa, and P. Sodano, Phys. Rev. D **72**, 094508 (2005).
[11] H. So, Prog. Theor. Phys. **73**, 528 (1985).
[12] H. So, Prog. Theor. Phys. **74**, 585 (1985).
[13] A. Coste and M. Luscher, Nucl. Phys. **B323**, 631 (1989).
[14] G. V. Dunne, arXiv:hep-th/9902115.
[15] R. D. Pisarski, Phys. Rev. D **34**, 3851 (1986).
[16] M. Henneaux and C. Teitelboim, Phys. Rev. Lett. **56**, 689 (1986).
[17] Y. Hosotani, Phys. Rev. Lett. **62**, 2785 (1989).
[18] S. Deser, L. Griguolo, and D. Seminara, Phys. Rev. Lett. **79**, 1976 (1997).
[19] S. Deser, L. Griguolo, and D. Seminara, Phys. Rev. D **57**, 7444 (1998).
[20] C. Fosco, G. Rossini, and F. Schaposnik, Phys. Rev. Lett. **79**, 1980 (1997).
[21] E. Nissimov and S. Pacheva, Phys. Lett. **157B**, 407 (1985).
[22] L. Alvarez-Gaume, S. Della Pietra, and G. W. Moore, Ann. Phys. (N.Y.) **163**, 288 (1985).
[23] S. Forte, Nucl. Phys. **B288**, 252 (1987).
[24] S. Forte, Nucl. Phys. **B301**, 69 (1988).
[25] Y. Kikukawa and H. Neuberger, Nucl. Phys. **B513**, 735 (1998).
[26] A. Hasenfratz and D. Toussaint, Nucl. Phys. **B371**, 539 (1992).
[27] H. Neuberger, Phys. Rev. D **57**, 5417 (1998).
[28] R. Narayanan and H. Neuberger, Phys. Rev. Lett. **71**, 3251 (1993).
[29] I. Sachs and A. Wipf, Helv. Phys. Acta **65**, 652 (1992).
[30] E. Witten, What We Can Hope To Prove About 3d Yang-Mills Theory, http://media.scgp.stonybrook.edu/presentations/20120117_3_Witten.pdf.
[31] R. Narayanan and J. Nishimura, Nucl. Phys. **B508**, 371 (1997).